Published in final edited form as:

Oncogene. 2018 August ; 37(33): 4599–4610. doi:10.1038/s41388-018-0289-x.

Restoring PUMA induction overcomes *KRAS*-mediated resistance to anti-EGFR antibodies in colorectal cancer

Kyle Knickelbein[1,2], **Jingshan Tong**[1,2], **Dongshi Chen**[1,2], **Yi-Jun Wang**[1,2], **Sandra Misale**[3,4], **Alberto Bardelli**[3], **Jian Yu**[1,5], and **Lin Zhang**[1,2,*]

[1]UMPC Hillman Cancer Center, Pittsburgh, PA, 15213, USA

[2]Department of Pharmacology and Chemical Biology, University of Pittsburgh School of Medicine, Pittsburgh, PA, 15213, USA

[3]Candiolo Cancer Institute-FPO, IRCCS; Department of Oncology, University of Torino, 10060 Candiolo (TO), Italy

[4]Program in Molecular Pharmacology, Memorial Sloan Kettering Cancer Center, New York, New York 10065, USA

[5]Department of Pathology, University of Pittsburgh School of Medicine, Pittsburgh, PA, 15213, USA

Abstract

Intrinsic and acquired resistance to anti-EGFR antibody therapy, frequently mediated by mutant or amplified *KRAS* oncogene, is a significant challenge in the treatment of colorectal cancer (CRC). However, the mechanism of *KRAS*-mediated therapeutic resistance is not well understood. In this study, we demonstrate that clinically used anti-EGFR antibodies, including cetuximab and panitumumab, induce killing of sensitive CRC cells through p73-dependent transcriptional activation of the pro-apoptotic Bcl-2 family protein PUMA. PUMA induction and p73 activation are abrogated in CRC cells with acquired resistance to anti-EGFR antibodies due to *KRAS* alterations. Inhibition of aurora kinases preferentially kills mutant *KRAS* CRC cells and overcomes *KRAS*-mediated resistance to anti-EGFR antibodies *in vitro* and *in vivo* by restoring PUMA induction. Our results suggest that PUMA plays a critical role in meditating the sensitivity of CRC cells to anti-EGFR antibodies, and that restoration of PUMA-mediated apoptosis is a promising approach to improve the efficacy of EGFR-targeted therapy.

Keywords

Colorectal cancer; PUMA; Anti-EGFR antibody; KRAS; Aurora kinase; Apoptosis

Correspondence: Lin Zhang, the UPCI Research Pavilion, Room 2.42a, UPMC Hillman Cancer Center, 5117 Centre Ave., Pittsburgh, PA 15213. Phone: (412) 623-1009. Fax: (412) 623-7778. zhanglx@upmc.edu.

Conflicts of Interest Statement

None declared.

Introduction

Colorectal cancer (CRC) is the second-leading cause of cancer-related death in the United States [1]. Nearly half of CRC patients ultimately develop metastatic disease with a five-year survival rate only ~14% [1]. Current therapeutic treatments of CRCs include conventional chemotherapy and recent targeted therapy, which often involves monoclonal antibodies against VEGF-A (e.g. bevacizumab) or epidermal growth factor receptor (EGFR) (e.g. cetuximab and panitumumab) [2]. Apoptosis induction has been implicated as a critical mechanism of targeted agents including anti-EGFR antibodies [3, 4]. Stress-induced apoptosis in mammalian cells is mediated by the Bcl-2 family proteins, which regulate cell death through a series of events, including permeabilization of the outer mitochondrial membrane, cytosolic release of cytochrome *c*, and activation of caspases [5]. However, the mechanisms by which anti-EGFR antibodies induce the death of CRC cells are not well characterized. Furthermore, anti-EGFR antibodies are effective only in a subset of CRC patients with wildtype *KRAS* or *BRAF*. Extended use of anti-EGFR antibodies almost invariably leads to acquired resistance due to selection of cells with mutant *KRAS, BRAF*, or other oncogenes [6, 7].

KRAS encodes a small GTPase that mediates signals from growth factor receptors to downstream PI3K/AKT and MEK/ERK effector pathways [8]. *KRAS* mutations, mostly at codons 12, 13, and 61, lock KRAS into a constitutively active GTP-bound form, resulting in hyperactive PI3K/AKT and RAF/MEK/ERK signaling [9], as well as resistance to anti-EGFR antibody therapy [10]. It has been shown that continuous exposure of sensitive CRC cells to anti-EGFR antibodies enriches a small fraction of cells with a *KRAS* mutation or genomic amplification, which underlies acquired resistance to anti-EGFR antibodies [11, 12]. However, the exact mechanisms by which mutant KRAS confers resistance to anti-EGFR therapy remains unclear. A variety of approaches have been explored to target mutant KRAS, such as directly inhibiting KRAS [13], and targeting KRAS downstream effector pathways [4, 14]. Despite these efforts, mutant KRAS has remained one of the most challenging oncology targets. Novel mechanistic insight and targeting approaches for KRAS-mediated resistance are urgently needed.

In this study, we identified p53-upregulated modulator of apoptosis (PUMA), a BH3-only Bcl-2 family member [15], as a critical mediator of apoptotic response to anti-EGFR antibodies in CRC cells. PUMA induction by anti-EGFR antibodies is mediated by the p53 homologue p73, and consistently abrogated in CRC cells with acquired resistance. We also found that inhibitors of aurora kinases can overcome the resistance to anti-EGFR antibodies by restoring PUMA induction, providing a rationale to improve the efficacy of EGFR-targeted therapy.

Results

PUMA induction mediates apoptotic response to anti-EGFR antibodies in CRC cells

To determine the response mechanisms, we analyzed several CRC cell lines that are exquisitely sensitive to anti-EGFR antibodies [16]. Treating DiFi and CCK-81 CRC cells with cetuximab or panitumumab suppressed cell growth in a dose-dependent manner (Fig.

1A and S1A) [11]. Cetuximab or panitumumab at 5 or 10 nM markedly induced cell death with characteristics of apoptosis, including nuclear condensation and fragmentation (Fig. 1B), Annexin V staining of plasma membrane (Fig. 1C), and activation of caspase-9 and caspases-3/7 (Fig. 1D, 1E, S1B, and S1C). We also detected permeabilization of mitochondrial outer membrane by MitoTracker staining (Fig. 1F), as well as cytosolic release of mitochondrial cytochrome *c* (Fig. 2G), following cetuximab or panitumumab treatment. The growth suppressive and apoptotic effects of the anti-EGFR antibodies were abolished by the pan-caspase inhibitor z-VAD-fmk (Fig. 1, A and G), indicating a critical role of apoptotic cell death.

To investigate how anti-EGFR antibodies induce apoptosis, we analyzed the expression of Bcl-2 proteins in DiFi cells treated with cetuximab or panitumumab. We found that the BH3-only protein PUMA is markedly induced at both the protein and mRNA levels in a time- and dose-dependent manner (Fig. 2A and S2A). Another BH3-only protein Bim was also induced by cetuximab treatment, but other Bcl-2 family members were not substantially changed (Fig. S2B). The induction of PUMA and Bim was also detected in other sensitive CRC cell lines, including CCK-81, HCA-46, and OXCO-2 cells (Fig. S2, C–E).

We then determined the role of PUMA and Bim in the apoptotic response to anti-EGFR antibodies. Knockdown of *PUMA* by siRNA abolished cetuximab- and panitumumab-induced viability loss, caspase activation, as well as nuclear fragmentation in DiFi cells (Fig. 2, B–E). In contrast, knockdown of *Bim* did not affect the killing of DiFi cells (Fig. S2F). PUMA depletion also suppressed cetuximab-induced permeabilization of the mitochondrial outer membrane and release of cytochrome *c* (Fig. 2, F and G). The requirement for PUMA rather than Bim for cetuximab- and panitumumab-induced apoptosis was verified in CCK-81 and HCA-46 cells (Fig. S2, G and H). These results suggest that PUMA induction plays a pivotal role in mediating the sensitivity and apoptotic response to anti-EGFR antibodies in CRC cells.

PUMA induction by anti-EGFR antibodies is mediated by p73

PUMA expression is regulated at the transcriptional level by several transcription factors, such as p53, FoxO3A, the p65 subunit of NF-κB, and the p53 homologue p73 [15]. Upon analyzing these transcription factors, we identified p73 as the key mediator of PUMA induction in response to EGFR antibodies. Increased p73 expression and Y99 phosphorylation were observed at 2–8 hr following cetuximab treatment (Fig. 3A, 3B, S3A and S3B), suggesting activating phosphorylation of p73 [17]. Enhanced binding of p73 to the *PUMA* promoter was detected by chromatin immunoprecipitation (ChIP) in cetuximab-treated cells (Fig. 3C). Knockdown of *p73* by siRNA substantially reduced PUMA induction, caspase-3 activation, and viability loss in cetuximab-treated DiFi cells (Fig. 3, A and D). In contrast, knockdown of *p53* did not affect PUMA induction by cetuximab (Fig. S3C), consistent with no change in p53 binding to the *PUMA* promoter (Fig. S3D). Knockdown of *FoxO3A* also had no effect on PUMA induction (Fig. S3E), despite its de-phosphorylation following cetuximab treatment (Fig. S3F).

We further investigated upstream events of p73 activation and PUMA induction. Treating DiFi cells with cetuximab potently suppressed phosphorylation of AKT and ERK1/2 (Fig.

3B), which are the key effectors of EGFR-mediated oncogenic signaling [18]. PUMA induction was detected in DiFi cells treated with the PI3K inhibitor pictilisib (GDC-0941) or dactolisib (NVP-BEZ235) (Fig. S3G), or the MEK inhibitor trametinib (Fig. S3H). Combined inhibition of PI3K and MEK further enhanced PUMA induction (Fig. S3H), suggesting that PUMA induction by cetuximab is mediated by both PI3K/AKT and MEK/ERK inhibition. It was previously shown that AKT negatively regulates p73 [17, 19]. Transfection of constitutively-active AKT suppressed cetuximab-induced p73 accumulation and phosphorylation, PUMA induction, as well as viability loss (Fig. 3, E and F). Our previous studies showed that PUMA can be induced by other transcriptional factors in response to ERK inhibition [20, 21]. Therefore, our findings support a model in which anti-EGFR antibodies inhibit PI3K/AKT and MEK/ERK to relieve their suppression on p73 and other transcription factors, which in turn bind to the *PUMA* promoter to activate *PUMA* transcription (Fig. 3G).

KRAS-mediated resistance to anti-EGFR antibodies abrogates PUMA induction by p73

Therapeutic resistance represents one of the most significant challenges for targeted therapies. CRCs with mutant or amplified *KRAS* are invariably insensitive to anti-EGFR antibody therapy [6, 22, 23]. Acquired resistance to anti-EGFR therapy is associated with enrichment of *KRAS*-mutant tumor cells [11, 12]. To elucidate the resistance mechanisms, we analyzed DiFi cells with acquired resistance to cetuximab [11, 14]. Compared to the parental DiFi cells, the cetuximab-resistant cells exhibited much reduced viability loss, caspase-3 activation, and Annexin V staining, following cetuximab or panitumumab treatment (Figs. 4A, 4B, and S4A). Consistent with previous studies [11, 14], the cetuximab-resistant DiFi cells had markedly elevated KRAS expression due to *KRAS* genomic amplification, and expressed a much lower level of total EGFR (Fig. 4C). In response to cetuximab, the resistant cells showed residual AKT and ERK phosphorylation, in contrast to complete AKT and ERK inhibition in the parental cells (Fig. 4C).

Analysis of Bcl-2 family proteins revealed that the induction of PUMA, but not Bim, by cetuximab was substantially reduced in the resistant cells compared to the parental cells (Fig. 4D). A similar observation on PUMA induction was made in the parental and panitumumab-resistant HCA-46 cells (Fig. S4C). Reduced PUMA induction coincided with lack of p73 accumulation and Y99 phosphorylation, but increased basal level of p73 in the resistant cells (Fig. 4E). Transfected exogenous p73 also lacked Y99 phosphorylation in the resistant cells (Fig. S4D). Furthermore, ChIP analysis revealed that cetuximab-induced binding of p73 to the *PUMA* promoter was abrogated in the resistant cells (Fig. 4F). These results suggest that lack of PUMA induction and p73 phosphorylation underlies reduced apoptosis in the resistant cells. Indeed, restoring PUMA with a PUMA-expressing adenovirus (Ad-PUMA) potently killed cetuximab-resistant DiFi cells, just as the parental cells (Fig. 4G). Treatment with the BH3 mimetic ABT-737 also markedly enhanced the effects of cetuximab in the resistant cells (Fig. S4E). Together, these results indicate that deficiencies in PUMA induction and p73 phosphorylation mediate resistance to anti-EGFR antibodies in CRC cells with oncogenic *KRAS*.

Aurora kinase inhibition preferentially kills *KRAS*-mutant CRC cells and restores sensitivity to anti-EGFR antibodies in the resistant cells

To overcome mutant-*KRAS*-mediated therapeutic resistance, we attempted to identify anticancer agents that can re-sensitize *KRAS*-mutant CRC cells by restoring PUMA induction. We showed that MEK inhibition could restore cetuximab sensitivity in *KRAS*-mutant CRC cells [11]. PI3K inhibition also modestly enhanced apoptosis and PUMA induction in cetuximab-resistant DiFi cells (Fig. S4F). To identify other agents that can effectively kill *KRAS*-mutant CRC cells, we analyzed isogenic CRC cells with either a mutant or wildtype (WT) *KRAS* allele generated by gene targeting [24]. Upon screening of a panel of anticancer agents including inhibitors of various oncogenic kinases, we found inhibitors of aurora kinases could preferentially kill *KRAS*-mutant cells compared to isogenic *KRAS*-WT cells (Fig. S5A). ZM-447439 (ZM), an inhibitor of aurora kinases A/B/C, induced significantly higher levels of growth inhibition (Fig. 5A), nuclear fragmentation (Fig. 5B), and caspase-3 activation (Fig. 5C), in DLD1 cells with only *KRAS* G13D mutant allele (G13D/-), compared to those with only WT allele (+/-). Alisertib (MLN8237), an inhibitor of aurora kinases A, had similar effects on *KRAS* G13D/− DLD1 cells (Fig. S5, B–E). The observed difference in apoptosis is not due to changes in cell proliferation, as the isogenic DLD1 cells analyzed have similar proliferation rates, and knockdown of mutant *KRAS* in G13D/− DLD1 cells did not affect cell proliferation and viability (Fig. S5F). Analysis of Bcl-2 family proteins revealed enhanced induction of the BH3-only proteins PUMA and Noxa in both the parental (G13D/+) and *KRAS*-mutant (G13D/-) cells, compared to the isogenic WT (+/-) cells (Fig. 5D). The increased killing of *KRAS*-mutant cells by ZM was largely due to enhanced PUMA induction, and abrogated in the isogenic *PUMA*-knockout HCT116 and DLD1 cells (Fig. S5G) [20]. However, ZM did not preferentially kill non-isogenic CRC cell lines with mutant *KRAS,* compared to those with WT *KRAS* (Fig. S5H).

The above findings prompted us to test whether aurora kinase inhibition could restore sensitivity to anti-EGFR antibodies in the resistant CRC cells with an alteration in *KRAS*. Indeed, a combination of ZM and cetuximab potently suppressed the growth of cetuximab-resistant DiFi cells (Fig. 5E), which was accompanied by enhanced nuclear fragmentation and caspase-3 activation (Fig. 5F). Consistent with the role of PUMA as a key mediator of sensitivity, the combination treatment restored PUMA induction in the resistant cells (Fig. 5G). The aurora kinase A inhibitor alisertib had similar effects on cetuximab-resistant DiFi cells (Fig. S6, A–C). In line with the proposed model (Fig. 3G), the ZM/cetuximab combination eliminated the residual phosphorylation of AKT and ERK in the resistant cells (Fig. 5H). Furthermore, ZM could also re-sensitize cetuximab-resistant OXCO-2 cells (Fig. S6D), and enhance the killing effect of cetuximab on *KRAS*-mutant CRC cell lines, including SW837, HCT116, LoVo, and HCT8 (Fig. S6E).

Aurora kinase inhibition overcomes *in vivo* resistance to anti-EGFR antibody therapy

To determine the *in vivo* efficacy of the combination treatment, parental and cetuximab-resistant OXCO-2 cells were used to establish xenograft tumors in nude mice. Tumor-bearing mice were treated with ZM, cetuximab, or their combination for 2 weeks, and monitored for tumor growth (Fig. 6A). Strikingly, the combination treatment almost

completely suppressed the growth of cetuximab-resistant tumors, while ZM or cetuximab alone only slightly inhibited tumor growth (Fig. 6, A–B). Analysis of tumor tissues collected at an early time point revealed that the combination treatment, but not single agent, restored PUMA induction in the resistant tumors (Fig. 6C). Furthermore, the ZM/cetuximab combination therapy strongly induced apoptosis as evidenced by markedly increased TUNEL and active caspase-3 staining, in both the parental and cetuximab-resistant OXCO-2 tumors (Fig. 6, D–E). Collectively, these results indicate that aurora kinase inhibitors can be used to overcome *KRAS*-mediated resistance to anti-EGFR antibodies by restoring PUMA-dependent apoptosis.

Discussion

Conventional chemotherapeutics including 5-fluorouracil, irinotecan, and oxaliplatin lack specificity and are ineffective against most CRCs [25]. Incorporation of targeted agents such as anti-EGFR antibodies has significantly improved CRC treatment [2]. Anti-EGFR antibodies suppress proliferation of most CRC cells, but also induce apoptosis with ambiguous mechanisms in some CRC cells [26, 27]. Our data show that inhibition of EGFR oncogenic signaling results in the accumulation and Y99 phosphorylation of p73, which in turn binds to the *PUMA* promoter to induce PUMA expression, leading to mitochondrial dysfunction and apoptosis induction. The induction of PUMA by p73 via AKT inhibition was also found to be involved in apoptosis induced by EGFR tyrosine kinase inhibitors (TKIs) in head and neck cancer cells [19]. The mechanism by which AKT inhibition promotes p73 activation remains to be determined. It has been shown that p73 expression is negatively regulated by AKT through the transcriptional co-activator YAP1 [17, 28]. c-Abl kinase promotes p73 Y99 phosphorylation in response to genotoxic stress [29]. It is likely that YAP1 and c-Abl are involved in regulating p73 phosphorylation and PUMA induction in response to anti-EGFR antibodies.

A number of previous studies showed that induction of BH3-only proteins is critical for initiating apoptosis in response to targeted drugs in different types of cancer cells. For example, Bim induction was found to be necessary for apoptosis in response to MEK or EGFR inhibition in non-small cell lung cancer (NSCLC) and melanoma cells [30, 31]. Bim also mediates apoptosis induced by combined inhibition of Bcl-X_L and MEK in *KRAS*-mutant CRC and lung cancer cells [32]. Bim and PUMA are both involved in apoptosis induced by MEK and PI3K inhibition in NSCLC cells [33]. In contrast, our results indicate that PUMA rather than Bim functions as a key mediator of apoptosis induced by anti-EGFR antibodies in sensitive CRC cells. The discrepancy could be explained by the stimulus- and cell-type-specific role of BH3-only proteins in apoptosis [34]. Although PUMA is required for apoptosis induced by different stimuli in CRC cells [15, 19, 20], it may have a less critical role than Bim or other BH3-only proteins in different types of cancer cells. Our study is also different from other studies on CRC cells as we analyzed CRC cell lines that are intrinsically sensitive to EGFR inhibition, instead of commonly used CRC cell lines which are often insensitive to EGFR inhibition alone; and we used anti-EGFR antibodies rather than EGFR TKIs or other small-molecule inhibitors to induce apoptosis.

Resistance to EGFR-targeted therapy represents a significant problem in the treatment of CRC patients. Retrospective analyses of clinical data and patient specimens revealed that alterations in the *KRAS* oncogene are largely responsible for the resistance to anti-EGFR antibodies [22, 35]. Several recent studies showed that a small fraction of pre-existing *KRAS*-mutant cells, which can be detected in circulating tumor DNA (ctDNA) from liquid biopsies, become enriched upon anti-EGFR antibody treatment, and eventually prevail leading to acquired resistance and disease relapse [36]. We show that acquired resistance to anti-EGFR antibodies can be caused by defective apoptosis due to lack of p73 and PUMA activation. It remains to be answered how p73 activity is compromised in the resistant cells, which might involve residual activities in AKT/ERK and/or other upstream kinases such as c-Abl.

Using isogenic CRC cells, we identified increased sensitivity of *KRAS*-mutant cells to aurora kinase inhibitors by restoring PUMA induction and the apoptotic response to anti-EGFR antibodies in the resistant cells with a mutant or amplified *KRAS*. The restored PUMA expression in the resistant cells by the combination treatment is likely due to the p65 subunit of NF-κB, which was shown to promote PUMA induction in response aurora kinase inhibition [20]. Previous synthetic lethal screens identified preferential killing of isogenic *KRAS*-mutant cells by the inhibitors of polo-like kinase 1 (PLK1) and the microtubule poison paclitaxel [37]. These observations, along with ours, suggest that CRC cells with *KRAS* alterations are addicted to hyperactive mitotic kinases, which lead to enhanced cell cycle progression and cell proliferation in cells with increased KRAS activity [8].

There is an unmet clinical need for targeting *KRAS*-mutant tumors to circumvent therapeutic resistance, and a variety of rational combination strategies have been explored. For example, MEK/EGFR dual inhibition has been shown to be effective against *KRAS*-mutant tumors [14]. A recent study showed that EGFR inhibition can increase the sensitivity to DNA damage [38], providing a rationale for combining anti-EGFR antibodies and DNA-damaging agents. Defective apoptosis is a hallmark of cancer and ubiquitously involved in therapeutic resistance [39]. Targeting defective apoptosis in tumor cells has recently emerged as an attractive therapeutic strategy with the recent FDA approval of the Bcl-2-selective inhibitor ABT-199 (Venetoclax) for the treatment of chronic lymphocytic leukemia (CLL) [40]. Our results suggest that targeting PUMA-mediated apoptosis by restoring PUMA expression or mimicking its functional BH3 domain is a promising approach for improving the efficacy of EGFR-targeted therapy in resistant tumor cells. The translational relevance of our findings needs to be further substantiated using additional anti-EGFR antibody resistant models including patient-derived xenograft (PDX) tumor models.

In summary, our study provides a novel insight on how EGFR inhibition triggers death of CRC cells through p73-mediated PUMA induction, which is blunted in resistant cells with *KRAS* alterations. Our results provide a rationale for further exploring aurora kinase inhibitors to improve the efficacy of EGFR-targeted therapy, especially in *KRAS*-altered tumors.

Materials and Methods

Cell culture and drug treatment

Human CRC cell lines, including parental and cetuximab-resistant DiFi, CCK-81, and OXCO-2, and parental and panitumumab-resistant HCA-46, were previously described [11, 14]. Cetuximab-resistant DiFi cells (R1 clone) were established by treating parental DiFi cells with a constant dose of cetuximab (0.35 μM) for one year [11]. Cetuximab-resistant OXCO-2 cells (R1 clone) and panitumumab-resistant HCA-46 cells were generated by continuous exposure of the parental cells to the drug at a concentration of 1.4 μM for 3–9 months [14]. Isogenic HCT116 and DLD1 cells with different *KRAS* genotypes [24] were obtained from Dr. Bert Vogelstein at Johns Hopkins University. CRC cell lines were tested for the absence of mycoplasma approximately every 6 months. All CRC cell lines were cultured in McCoy's 5A modified media (Invitrogen, Carlsbad, CA, USA), and maintained in a non-humidified incubator at 37°C with the addition of 5% CO_2. Cell culture media were supplemented with 10% FBS (HyClone, Logan, UT, USA) and 1% penicillin-streptomycin consisting of 100 units/mL penicillin and 100 μg/mL streptomycin (Invitrogen).

Cells were plated at 20–30% density in 12-well plates for drug treatment. Anticancer agents utilized include: cetuximab and panitumumab (supplied through UPCI Pharmacy), dactolisib (NVP-BEZ235), free base, pictilisib (GDC-0941), free base, sorafenib, 17-AAG, PF-02341066 (crizotinib), vandetanib, erlotinib hydrochloride salt, dasatinib free base, tozasertib free base, (LC Laboratories, Woburn, MA,USA), ZM-447439, MG-132, volasertib (BI 6727), ABT-737, alisertib (Selleck Chemicals, Houston, TX, USA), sunitinib (Cayman Chemical, Ann Arbor, MI, USA), trametinib (ApexBio, Boston, MA), and z-Val-Ala-DL-Asp(OMe)-fluoromethylketone (z-VAD-fmk) (Bachem, Torrance, CA, USA). Antibodies were diluted in PBS, and chemical agents in DMSO (Sigma, St. Louis, MO, USA).

Analysis of cell viability and apoptosis

Cell viability was analyzed by MTS and CellTiter-Glo assays as previously described [41]. For crystal violet staining, attached cells were washed with HBSS and stained by incubating cells at room temperature with a 0.05% crystal violet solution containing 3.7% paraformaldehyde prepared in distilled water. Apoptosis was analyzed by staining floating and attached cells with Hoechst 33258 (Invitrogen) and by counting condensed and fragmented nuclei, which were divided by the total number of cells counted to obtain the final percentages. Unless otherwise specified, each condition was analyzed in duplicate per experiment counting at least 300 cells per sample. Apoptosis was also analyzed by Annexin-V/PI staining, Caspase-3/-7 activity Assay, and mitochondrial outer membrane permeabilization as previously described [41, 42].

Transfection and adenovirus infection

Cells were transfected with Lipofectamine 2000 (Invitrogen) according to the manufacturer's instructions. Briefly, cells were plated at 20–30% density in 12-well plates 24 hr prior to transfection. siRNAs were transfected in 1× Opti-MEM (Invitrogen) with 200 or 400 pmol of siRNA per well of a 12-well plate for 4 hr before the addition of McCoy's

5A medium. The sequences utilized for each siRNA are described in Table S1. For plasmid transfection, the equivalent of 0.2 μg of plasmid per well of a 12-well plate was utilized. Plasmids utilized included N-terminal HA-tagged pcDNA3.1 empty vector (control plasmid), HA-tagged p73α in a pcDNA3 vector [42], and N-terminal myristolated, constitutively-active AKT1 in a pUSEamp(+) vector (#21–151, EMD Millipore, Burlington, MA, USA). Drug treatments were performed approximately 24 hr following transfection. For adenovirus infection, cells were infected at either 20 or 40 MOI for 24 hr with a GFP-tagged PUMA-expressing adenovirus (Ad-PUMA) described previously [43].

Western blotting

Western blotting was performed as previously described [41] using antibodies against: β-Actin (A5441, Sigma), cleaved caspase-3 (#9661, Cell Signaling, Danvers, MA, USA), cleaved caspase-9 (#9502, Cell Signaling), Mcl-1 (#559027, BD Biosciences, San Jose, CA, USA), Bax (#610983, BD Biosciences), Bid (#2002, Cell Signaling), Bcl-xL (#610212, BD Biosciences), Bim (#2819, Cell Signaling), Bcl-2 (#M0887, Agilent DAKO, Santa Clara, CA, USA), cytochrome *c* (sc-7159, Santa Cruz Biotechnology, Santa Cruz, CA, USA), COX IV (A21348, Invitrogen), PUMA [44], Bak (#06–536, EMD Millipore), Noxa (#OP180, EMD Millipore), p73 (A300–126A, Bethyl Laboratories, Montgomery, TX, USA), p-p73 (#4665, Cell Signaling), p-AKT (#4058, Cell Signaling), total AKT (#9272, Cell Signaling), p-ERK1/2 (#4376, Cell Signaling), total ERK1/2 (#9102, Cell Signaling), p-FoxO3A (#9464, Cell Signaling), total FoxO3A (07–702, EMD Millipore), p53 (sc-126, Santa Cruz), p-EGFR (#2234, Cell Signaling), total EGFR (#610016, BD Biosciences), KRAS (sc-30, Santa Cruz), p-Aurora A/B/C (#2914, Cell Signaling), total Aurora A (#4718, Cell Signaling), total Aurora B (#3094, Cell Signaling), and HA (#12CA5, Roche, Indianapolis, IN, USA).

Reverse-transcription (RT) and quantitative PCR

RNA extracts were prepared from cells using the Quick-RNA MiniPrep kit (Zymo Research, Irvine, CA, USA) according to the manufacturer's instructions. cDNA was prepared from total RNA using SuperScript III Reverse Transcriptase (Invitrogen). Following reverse transcription, quantitative PCR was performed using a cycling profile consisting of 95°C for 2 minutes (Stage I), 30 cycles of 95°C for 20 seconds, 58°C for 30 seconds, and 70°C for 30 seconds (Stage II), and 65°C for 5 seconds (Stage III). Fold changes were determined by subtracting Cq values of the loading control from the Cq values of the gene of interest. The results were normalized to untreated controls. PCR primers are listed in Table S2.

Immunoprecipitation

Cells were lysed in buffer consisting of 50 mM Tris, 150 mM NaCl, 1% NP-40, 1 mM EDTA, and 10% glycerol prepared in distilled water. The final pH was adjusted to 7.5. Protease-inhibitor tablets (Roche) were also added to the buffer prior to lysis. Cell lysates were incubated with EZview Red Protein G Affinity Gel (Sigma) beads utilizing an antibody against p-p73 (#4665, Cell Signaling). Following an overnight incubation at 4°C, the bead-protein complex was washed, lysed in 2× Laemmli buffer and analyzed by Western blot.

Xenograft tumor experiments

The described animal experiments were approved by the University of Pittsburgh Institutional Animal Care and Use Committee (IACUC). Female Nu/Nu mice (Charles River, Wilmington, MA, USA) aged 5–6 weeks were utilized for all xenograft experiments. Mice were maintained on-site in a sterile environment in micro-isolator cages and were given continuous access to water and chow. Following a one-week rest period, mice were injected subcutaneously with 5×10^6 OXCO-2 parental and cetuximab-resistant cells (R1 clone) on two flanks. After one week of tumor growth, treatments were initiated by intraperitoneal (i.p.) injection with 40 mg/kg ZM-447439 in 10% DMSO every other day, 0.8 mg of cetuximab every 3 to 4 days, or their combination. Treatments were terminated either at day 5 (for immunostaining) or at day 15 (for tumor volume measurement). Control mice received 10% DMSO opposite ZM-443439 treatment and combination treatment, or HBSS opposite cetuximab treatment. 10% DMSO and ZM-447439 preparations were diluted in a solution of filter-sterilized 50% HBSS/50% PEG300. Tumor growth was measured every other day by two not-blinded investigators with calipers, and tumor volumes were calculated using the formula $0.5 \times \text{length} \times \text{width}^2$. After the mice were sacrificed, tumors were excised and prepared for immunostaing by fixing in 10% formalin followed by paraffin embedding. As all treated animals were analyzed, no randomization was needed.

Statistical Analysis

For animal experiments, the sample size (n=6 in each group) was estimated based on our previous experience working with ZM-447439 on xenograft tumors [20]. The statistical significance between two groups was determined with Student's t-test, whereas the comparisons of multiple groups were carried out by one-way ANOVA, followed by Bonferroni's post-test using GraphPad Prism IV software. A probability value of $*P < 0.05$ was considered to be significant. Error bars in the figures represent the standard error of the means.

Supplementary Material

Refer to Web version on PubMed Central for supplementary material.

Acknowledgments

The authors thank our lab members for critical reading. This work is supported by U.S. National Institute of Health grants (R01CA106348, R01CA172136, R01CA203028, and R01CA217141 to L.Z.; U19AI068021 and R01CA215481 to J.Y.). K.K. was supported by a fellowship from the Cotswold Foundation and the Department of Pharmacology & Chemical Biology, University of Pittsburgh School of Medicine. This project used the UPMC Hillman Cancer Center shared facilities that were supported in part by award P30CA047904.

Abbreviations

ChIP	chromatin immunoprecipitation
CRC	colorectal cancer
EGFR	epidermal growth factor receptor
IP	immunoprecipitation

KO	knockout
NSCLC	non-small cell lung cancer
PUMA	p53-upregulated modulator of apoptosis
RT-PCR	reverse transcriptase-polymerase chain reaction
siRNA	small interfering RNA
TKIs	tyrosine kinase inhibitors
TUNEL	terminal deoxynucleotidyl transferase mediated dUTP nick end labeling
z-VAD	carbobenzoxy-valyl-alanyl-aspartyl-[O-methyl]-fluoromethylketone

References

1. Siegel RL, Miller KD, Jemal A. Cancer Statistics, 2017. CA Cancer J Clin. 2017; 67:7–30. [PubMed: 28055103]
2. Chu E. An update on the current and emerging targeted agents in metastatic colorectal cancer. Clinical colorectal cancer. 2012; 11:1–13. [PubMed: 21752724]
3. Zhang L, Yu J. Role of apoptosis in colon cancer biology, therapy, and prevention. Curr Colorectal Cancer Rep. 2013; 9:331–40.
4. Misale S, Bozic I, Tong J, Peraza-Penton A, Lallo A, Baldi F, et al. Vertical suppression of the EGFR pathway prevents onset of resistance in colorectal cancers. Nat Commun. 2015; 6:8305. [PubMed: 26392303]
5. Bhola PD, Letai A. Mitochondria-Judges and Executioners of Cell Death Sentences. Mol Cell. 2016; 61:695–704. [PubMed: 26942674]
6. Bardelli A, Siena S. Molecular mechanisms of resistance to cetuximab and panitumumab in colorectal cancer. J Clin Oncol. 2010; 28:1254–61. [PubMed: 20100961]
7. Banck MS, Grothey A. Biomarkers of Resistance to Epidermal Growth Factor Receptor Monoclonal Antibodies in Patients with Metastatic Colorectal Cancer. Clin Cancer Res. 2009; 15:7492–501. [PubMed: 20008849]
8. Pylayeva-Gupta Y, Grabocka E, Bar-Sagi D. RAS oncogenes: weaving a tumorigenic web. Nat Rev Cancer. 2011; 11:761–74. [PubMed: 21993244]
9. Karnoub AE, Weinberg RA. Ras oncogenes: split personalities. Nat Rev Mol Cell Biol. 2008; 9:517–31. [PubMed: 18568040]
10. Martini M, Vecchione L, Siena S, Tejpar S, Bardelli A. Targeted therapies: how personal should we go? Nat Rev Clin Oncol. 2012; 9:87–97.
11. Misale S, Yaeger R, Hobor S, Scala E, Janakiraman M, Liska D, et al. Emergence of KRAS mutations and acquired resistance to anti-EGFR therapy in colorectal cancer. Nature. 2012; 486:532–6. [PubMed: 22722830]
12. Diaz LA Jr, Williams RT, Wu J, Kinde I, Hecht JR, Berlin J, et al. The molecular evolution of acquired resistance to targeted EGFR blockade in colorectal cancers. Nature. 2012; 486:537–40. [PubMed: 22722843]
13. Ostrem JM, Peters U, Sos ML, Wells JA, Shokat KM. K-Ras(G12C) inhibitors allosterically control GTP affinity and effector interactions. Nature. 2013; 503:548–51. [PubMed: 24256730]
14. Misale S, Arena S, Lamba S, Siravegna G, Lallo A, Hobor S, et al. Blockade of EGFR and MEK intercepts heterogeneous mechanisms of acquired resistance to anti-EGFR therapies in colorectal cancer. Sci Transl Med. 2014; 6:224ra26.
15. Yu J, Zhang L. PUMA, a potent killer with or without p53. Oncogene. 2008; 27(Suppl 1):S71–83. [PubMed: 19641508]

16. Medico E, Russo M, Picco G, Cancelliere C, Valtorta E, Corti G, et al. The molecular landscape of colorectal cancer cell lines unveils clinically actionable kinase targets. Nat Commun. 2015; 6:7002. [PubMed: 25926053]
17. Conforti F, Sayan AE, Sreekumar R, Sayan BS. Regulation of p73 activity by post-translational modifications. Cell death & disease. 2012; 3:e285. [PubMed: 22419114]
18. Knickelbein K, Zhang L. Mutant KRAS as a critical determinant of the therapeutic response of colorectal cancer. Genes & Diseases. 2015; 2:4–12. [PubMed: 25815366]
19. Sun Q, Ming L, Thomas SM, Wang Y, Chen ZG, Ferris RL, et al. PUMA mediates EGFR tyrosine kinase inhibitor-induced apoptosis in head and neck cancer cells. Oncogene. 2009; 18:2348–57.
20. Sun J, Knickelbein K, He K, Chen D, Dudgeon C, Shu Y, et al. Aurora kinase inhibition induces PUMA via NF-kappaB to kill colon cancer cells. Mol Cancer Ther. 2014; 13:1298–308. [PubMed: 24563542]
21. Dudgeon C, Peng R, Wang P, Sebastiani A, Yu J, Zhang L. Inhibiting oncogenic signaling by sorafenib activates PUMA via GSK3beta and NF-kappaB to suppress tumor cell growth. Oncogene. 2012; 31:4848–58. [PubMed: 22286758]
22. Karapetis CS, Khambata-Ford S, Jonker DJ, O'Callaghan CJ, Tu D, Tebbutt NC, et al. K-ras mutations and benefit from cetuximab in advanced colorectal cancer. N Engl J Med. 2008; 359:1757–65. [PubMed: 18946061]
23. Amado RG, Wolf M, Peeters M, Van Cutsem E, Siena S, Freeman DJ, et al. Wild-type KRAS is required for panitumumab efficacy in patients with metastatic colorectal cancer. J Clin Oncol. 2008; 26:1626–34. [PubMed: 18316791]
24. Yun J, Rago C, Cheong I, Pagliarini R, Angenendt P, Rajagopalan H, et al. Glucose deprivation contributes to the development of KRAS pathway mutations in tumor cells. Science. 2009; 325:1555–9. [PubMed: 19661383]
25. Meyerhardt JA, Mayer RJ. Systemic therapy for colorectal cancer. N Engl J Med. 2005; 352:476–87. [PubMed: 15689586]
26. Lu Y, Li X, Liang K, Luwor R, Siddik ZH, Mills GB, et al. Epidermal growth factor receptor (EGFR) ubiquitination as a mechanism of acquired resistance escaping treatment by the anti-EGFR monoclonal antibody cetuximab. Cancer Res. 2007; 67:8240–7. [PubMed: 17804738]
27. Kasper S, Breitenbuecher F, Reis H, Brandau S, Worm K, Kohler J, et al. Oncogenic RAS simultaneously protects against anti-EGFR antibody-dependent cellular cytotoxicity and EGFR signaling blockade. Oncogene. 2013; 32:2873–81. [PubMed: 22797062]
28. Strano S, Munarriz E, Rossi M, Castagnoli L, Shaul Y, Sacchi A, et al. Physical interaction with Yes-associated protein enhances p73 transcriptional activity. J Biol Chem. 2001; 276:15164–73. [PubMed: 11278685]
29. Tsai KK, Yuan ZM. c-Abl stabilizes p73 by a phosphorylation-augmented interaction. Cancer Res. 2003; 63:3418–24. [PubMed: 12810679]
30. Cragg MS, Kuroda J, Puthalakath H, Huang DC, Strasser A. Gefitinib-induced killing of NSCLC cell lines expressing mutant EGFR requires BIM and can be enhanced by BH3 mimetics. PLoS Med. 2007; 4:1681–89. discussion 90. [PubMed: 17973573]
31. Cragg MS, Jansen ES, Cook M, Harris C, Strasser A, Scott CL. Treatment of B-RAF mutant human tumor cells with a MEK inhibitor requires Bim and is enhanced by a BH3 mimetic. J Clin Invest. 2008; 118:3651–9. [PubMed: 18949058]
32. Corcoran RB, Cheng KA, Hata AN, Faber AC, Ebi H, Coffee EM, et al. Synthetic lethal interaction of combined BCL-XL and MEK inhibition promotes tumor regressions in KRAS mutant cancer models. Cancer Cell. 2013; 23:121–8. [PubMed: 23245996]
33. Hata AN, Yeo A, Faber AC, Lifshits E, Chen Z, Cheng KA, et al. Failure to induce apoptosis via BCL-2 family proteins underlies lack of efficacy of combined MEK and PI3K inhibitors for KRAS-mutant lung cancers. Cancer Res. 2014; 74:3146–56. [PubMed: 24675361]
34. Giam M, Huang DC, Bouillet P. BH3-only proteins and their roles in programmed cell death. Oncogene. 2008; 27(Suppl 1):S128–36. [PubMed: 19641498]
35. Lievre A, Bachet JB, Le Corre D, Boige V, Landi B, Emile JF, et al. KRAS mutation status is predictive of response to cetuximab therapy in colorectal cancer. Cancer Res. 2006; 66:3992–5. [PubMed: 16618717]

36. Siravegna G, Mussolin B, Buscarino M, Corti G, Cassingena A, Crisafulli G, et al. Clonal evolution and resistance to EGFR blockade in the blood of colorectal cancer patients. Nat Med. 2015; 21:795–801. [PubMed: 26030179]

37. Luo J, Emanuele MJ, Li D, Creighton CJ, Schlabach MR, Westbrook TF, et al. A genome-wide RNAi screen identifies multiple synthetic lethal interactions with the Ras oncogene. Cell. 2009; 137:835–48. [PubMed: 19490893]

38. Lee HJ, Lan L, Peng G, Chang WC, Hsu MC, Wang YN, et al. Tyrosine 370 phosphorylation of ATM positively regulates DNA damage response. Cell Res. 2015; 25:225–36. [PubMed: 25601159]

39. Hanahan D, Weinberg RA. Hallmarks of cancer: the next generation. Cell. 2011; 144:646–74. [PubMed: 21376230]

40. Del Poeta G, Postorino M, Pupo L, Del Principe MI, Dal Bo M, Bittolo T, et al. Venetoclax: Bcl-2 inhibition for the treatment of chronic lymphocytic leukemia. Drugs of today. 2016; 52:249–60. [PubMed: 27252989]

41. Brown MF, Leibowitz BJ, Chen D, He K, Zou F, Sobol RW, et al. Loss of Caspase-3 sensitizes colon cancer cells to genotoxic stress via RIP1-dependent necrosis. Cell death & disease. 2015; 6:e1729. [PubMed: 25906152]

42. Chen D, Ming L, Zou F, Peng Y, Van Houten B, Yu J, et al. TAp73 promotes cell survival upon genotoxic stress by inhibiting p53 activity. Oncotarget. 2014; 5:8107–22. [PubMed: 25237903]

43. Ming L, Wang P, Bank A, Yu J, Zhang L. PUMA dissociates Bax and BCL-XL to induce apoptosis in colon cancer cells. J Biol Chem. 2006; 281:16034–42. [PubMed: 16608847]

44. Yu J, Wang Z, Kinzler KW, Vogelstein B, Zhang L. PUMA mediates the apoptotic response to p53 in colorectal cancer cells. Proc Natl Acad Sci U S A. 2003; 100:1931–6. [PubMed: 12574499]

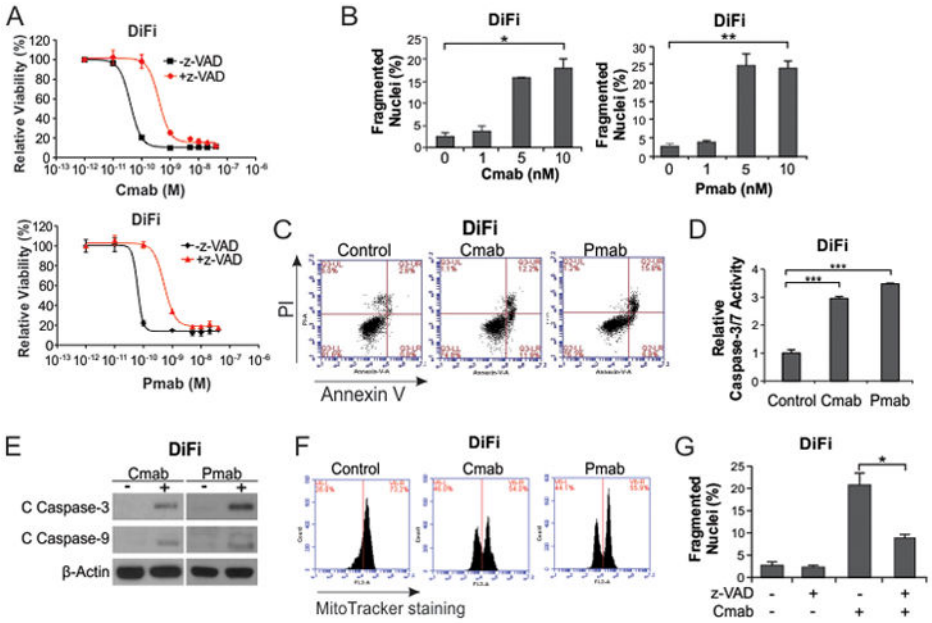

Figure 1. Anti-EGFR antibodies induce mitochondria-dependent apoptosis in sensitive CRC cells

(A) MTS analysis of DiFi colon cancer cells treated with cetuximab (Cmab) or panitumumab (Pmab) at the indicated doses for 72 hr. For comparison, DiFi cells pre-treated with 10 μM z-VAD-fmk (z-VAD) for 1 hr were also analyzed. **(B)** Apoptosis in DiFi cells treated Cmab or Pmab at the indicated doses for 72 hr was analyzed by counting condensed and fragmented nuclei after nuclear staining with Hoechst 33258. **(C)** Apoptosis in DiFi cells treated 10 nM Cmab or Pmab for 72 hr was analyzed by Annexin V/PI staining followed by flow cytometry. **(D)** Caspase-3/7 activity in DiFi cells treated with 10 nM Cmab or Pmab for 24 hr was measured using the Caspase-3/-7 Activation kit. **(E)** Western blotting of cleaved (C) caspase-3 and caspase-9 in DiFi cells treated as in (D). **(F)** Mitochondrial membrane integrity in DiFi cells treated with 10 nM of Cmab or Pmab for 72 hr was analyzed by MitoTracker Red CMXRos staining followed by flow cytometry. **(G)** DiFi cells with or without pre-treatment with 10 μM z-VAD-fmk (z-VAD) for 1 hr were treated with 10 nM Cmab for 72 hr. Apoptosis was analyzed as in (B). Results in (A), (B), (D) and (G) were expressed as means ± s.e.m. of triplicates in two independent experiments. *****, $P<0.05$; ******, $P<0.01$; *******, $P<0.001$

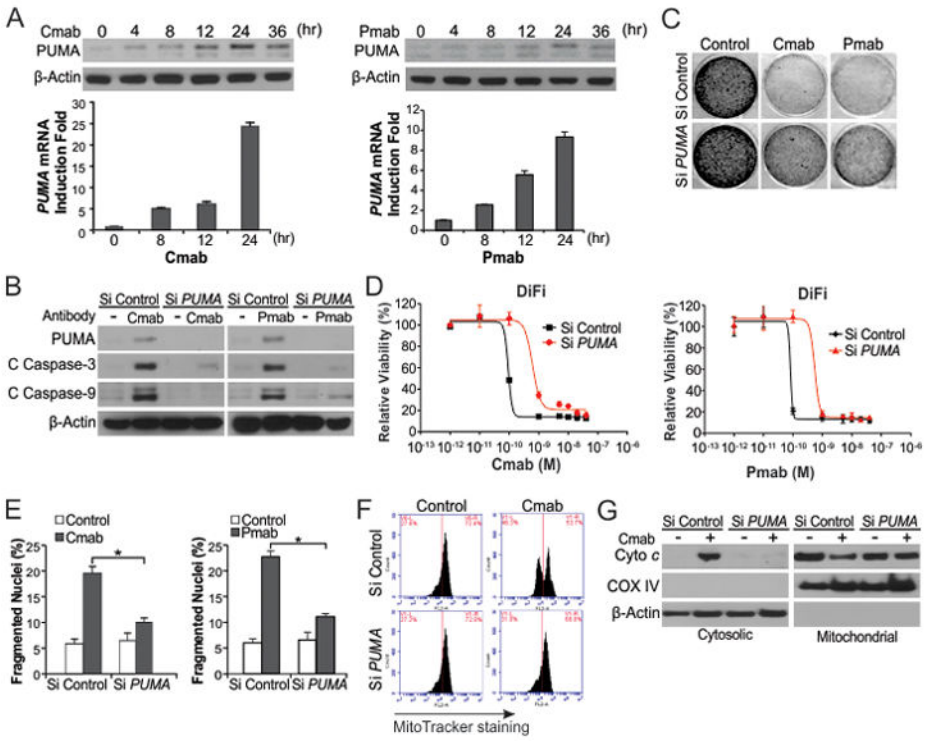

Figure 2. PUMA is a critical mediator of the apoptotic response to anti-EGFR antibodies

(A) DiFi cells were treated with 10 nM cetuximab (Cmab) or panitumumab (Pmab). *Upper,* western blotting of PUMA at indicated time points after treatment. *Lower,* real-time RT-PCR analysis of *PUMA* mRNA expression at indicated time points after treatment. **(B)** Western blotting of PUMA, cleaved (C) caspase-3, and caspase-9 in DiFi cells transfected with control scrambled or *PUMA* siRNA for 24 hr and treated with 10 nM Cmab or Pmab for 24 hr. **(C)** Crystal violet staining of DiFi cells transfected with siRNA as in (B), re-plated, and treated with 10 nM Cmab or Pmab for 48 hr. **(D)** MTS analysis of DiFi cells transfected with siRNA as in (B), re-plated, and treated with Cmab or Pmab at the indicated doses for 72 hr. **(E)** Apoptosis in DiFi cells transfected and treated as in (D) was analyzed by counting condensed and fragmented nuclei after nuclear staining with Hoechst 33258. **(F)** Mitochondrial membrane integrity in DiFi cells transfected and treated with Cmab as in (D) was analyzed by MitoTracker Red CMXRos staining followed by flow cytometry. **(G)** Cytochrome *c* (Cyto *c*) release in DiFi cells transfected and treated with Cmab as in (D) was analyzed by Western blotting of mitochondrial and cytosolic fractions isolated from treated cells. β-Actin and cytochrome oxidase subunit IV (COX IV) were used as a control for loading and fractionation, respectively. Results in (A), (D), and (E) were expressed as means ± s.e.m. of triplicates in two independent experiments. *****, $P<0.05$.

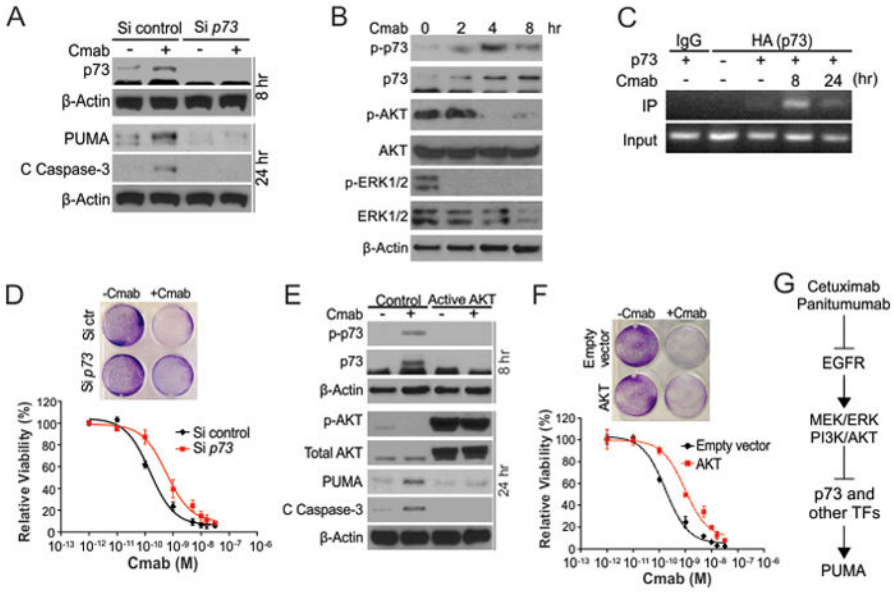

Figure 3. PUMA induction by anti-EGFR antibodies is mediated by p73

(A) DiFi cells transfected with control scrambled or *p73* siRNA for 24 hr were re-plated and treated with 10 nM cetuximab (Cmab). Expression of p73 at 8 hr, and PUMA and cleaved (C) caspase-3 at 24 hr after cetuximab treatment was analyzed by western blotting. Cells without siRNA transfection and re-plating were used as the control for analyzing p73 at 8r after treatment. **(B)** Western blotting of indicated proteins in DiFi cells treated 10 nM cetuximab at the indicated time points. Phospho-p73 (p-p73, Y99); phospho-AKT (p-AKT, S473); phospho-ERK1/2 (p-ERK1/2, T202/Y204). **(C)** DiFi cells transfected with either a control empty vector or a HA-p73α construct were treated with 10 nM Cmab for the indicated times. Binding of transfected p73α to the *PUMA* promoter was analyzed by chromatin immunoprecipitation (ChIP) using anti-HA antibody with IgG as control, followed by PCR amplification and analysis of PCR products by agarose gel electrophoresis. **(D)** Crystal violet staining (upper panel) and MTS analysis (lower panel) of DiFi cells transfected with siRNA as in (A) and treated with Cmab at the indicated doses for 72 hr. **(E)** Western blotting of indicated proteins in DiFi cells transfected with control empty vector or constitutively active AKT for 6 hr, and then treated with 10 nM cetuximab for 8 or 24 hr. **(F)** Crystal violet staining (upper panel) and MTS analysis (lower panel) of DiFi cells transfected as in (E) and treated with Cmab at the indicated doses for 72 hr. **(G)** A model of PUMA induction by anti-EGFR antibodies.

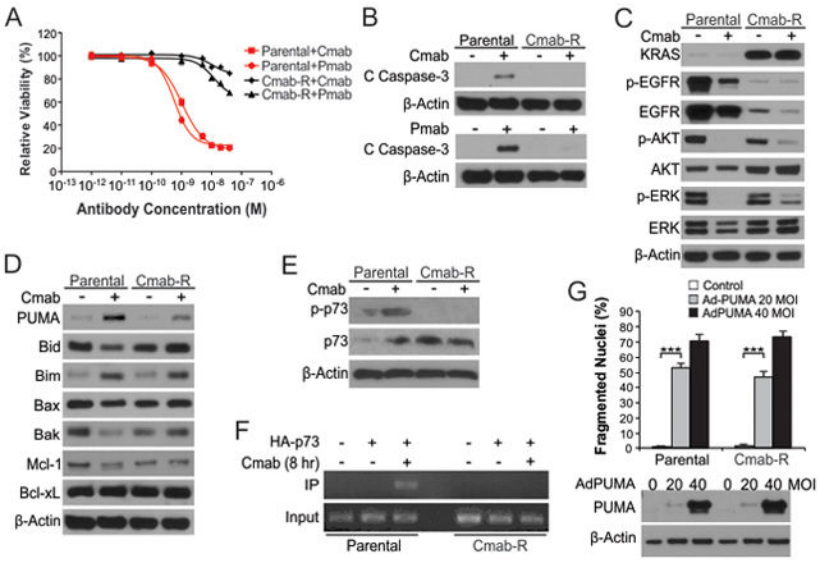

Figure 4. *KRAS*-mediated resistance to anti-EGFR antibodies abrogates PUMA induction

(A) MTS analysis of parental (red) and cetuximab-resistant (Cmab-R, black) DiFi cells treated with cetuximab (Cmab) or panitumumab (Pmab) at the indicated doses for 72 hr. **(B)** Western blotting of cleaved (C) caspase-3 in the parental and Cmab-R DiFi cells treated with 10 nM of Cmab or Pmab for 24 hr. **(C)** Western blotting of indicated proteins in the parental and Cmab-R DiFi cells. Lysates of Cmab-R DiFi cells were prepared from cells cultured in medium with 10 nM cetuximab (Cmab+), or without cetuximab (Cmab-) for 6 days. p-EGFR (Y1068); p-AKT (S473); p-ERK1/2 (T202/Y204). **(D)** Western blotting of indicated Bcl-2 family proteins in the parental and Cmab-R DiFi cells treated with 10 nM of Cmab for 24 hr. **(E)** Western blotting of phosphorylated (p-p73, Y99) and total p73 in the parental and Cmab-R DiFi cells treated with 10 nM Cmab for 8 hr. **(F)** Parental and Cmab-R DiFi cells transfected with control empty or HA-p73α-expressing vector were treated with 10 nM cetuximab for 8 hr. Binding of transfected p73α to the *PUMA* promoter was analyzed by chromatin immunoprecipitation (ChIP) using anti-HA antibody, followed by PCR amplification and analysis of PCR products by agarose gel electrophoresis. **(G)** Parental and Cmab-R DiFi cells were infected with EGFP-PUMA-expressing adenovirus (Ad-PUMA) at the indicated MOI for 24 hr. *Upper,* analysis of apoptosis by nuclear fragmentation; *lower*, western blotting of PUMA. Results were expressed as means ± s.e.m. of triplicates in two independent experiments. ***P<0.001.

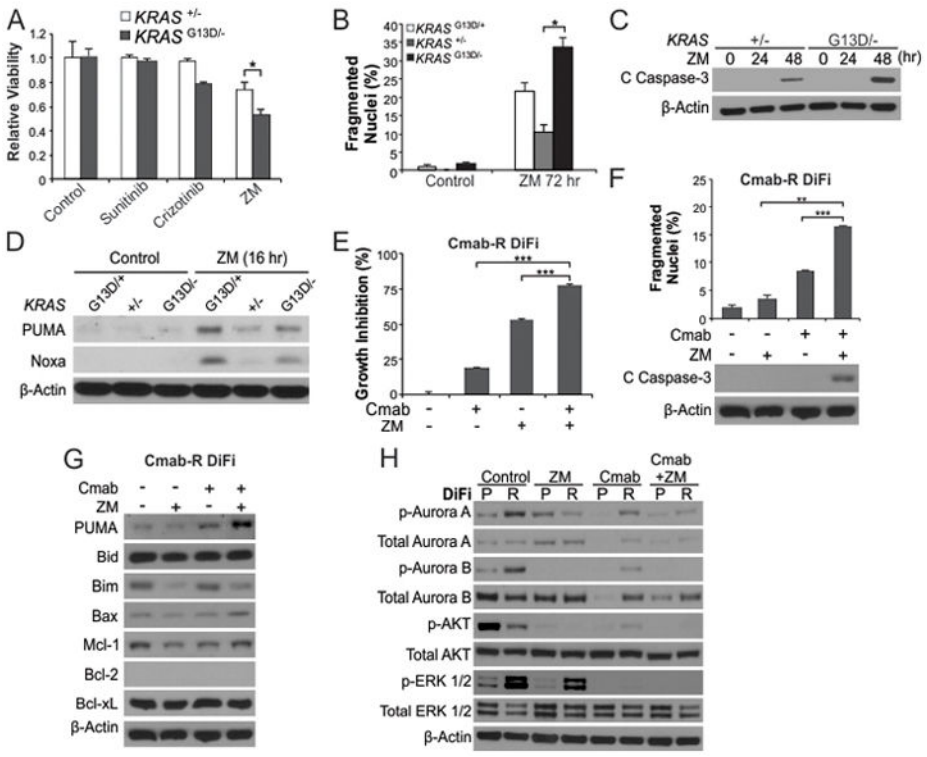

Figure 5. Aurora kinase inhibition overcomes *KRAS*-mediated resistance to anti-EGFR antibodies by restoring PUMA induction

(A) MTS analysis of isogenic DLD1 cells with +/− or G13D/− *KRAS* genotype treated with 7.5 μM sunitinib, 12 μM crizotinib, or 15 μM ZM-447439 (ZM) for 48 hr. **(B)** DLD1 cells with indicated *KRAS* genotypes were treated with 15 μM ZM. Apoptosis at the indicated time points was analyzed by counting condensed and fragmented nuclei after nuclear staining with Hoechst 33258. **(C)** Western blotting of cleaved (C) caspase-3 in DLD1 cells with the indicated *KRAS* genotypes treated with 15 μM ZM for 24 or 48 hr. **(D)** Western blotting of PUMA and Noxa in DLD1 cells with the indicated *KRAS* genotypes treated with 15 μM ZM for 16 hr. **(E)** Cetuximab-resistant (Cmab-R) DiFi cells were treated for 48 hr with 10 nM cetuximab, 15 μM ZM, or their combination. Growth inhibition was assessed using the CellTiter-Glo assay. **(F)** Cmab-R DiFi cells were treated with 10 nM cetuximab, 15 μM ZM, or their combination. Apoptosis was analyzed by nuclear fragmentation as in (B) after treatment for 72 hr (upper panel), and by western blotting of cleaved (C) caspase-3 after treatment for 24 hr (lower panel). **(G)** Western blotting of indicated Bcl-2 family proteins in Cmab-R DiFi cells treated for 24 hr with 10 nM cetuximab, 15 μM ZM, or their combination. **(H)** Western blotting of indicated proteins in parental (P) and cetuximab-resistant (R) DiFi cells treated with 15 μM ZM-447439 (ZM), 10 nM cetuximab, or their combination for 24 hr. p-Aurora A (T288); p-Aurora B (T232); p-AKT (S473); p-ERK1/2 (T202/Y204). Results in (A), (B), (E), and (F) were expressed as means ± s.e.m. of triplicates in two independent experiments. *, $P<0.05$; **, $P<0.01$; ***, $P<0.001$.

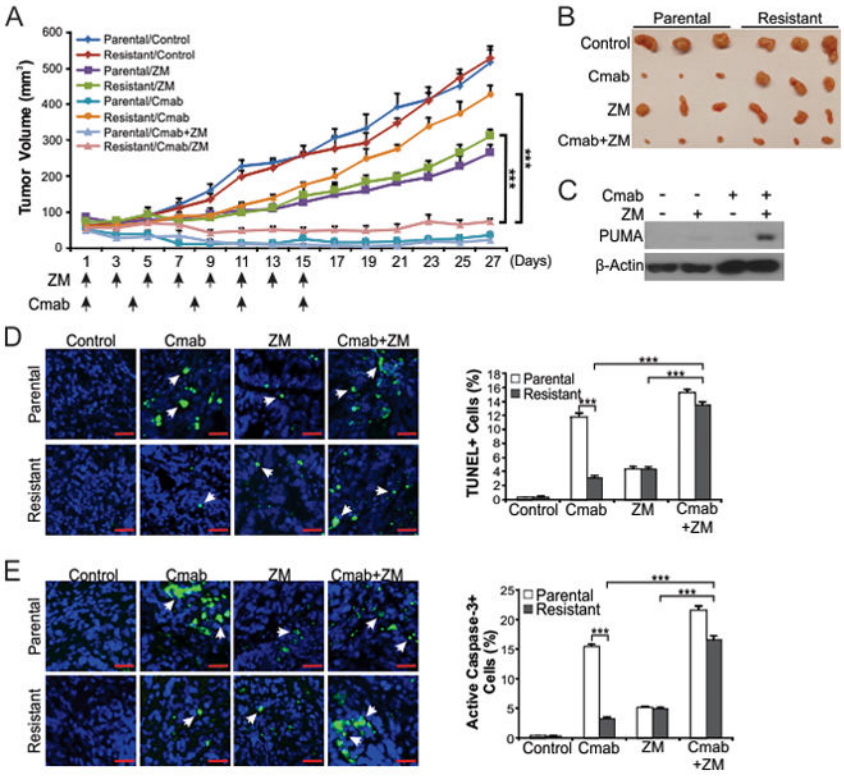

Figure 6. Aurora kinase inhibition overcomes *KRAS*-mediated resistance to anti-EGFR antibodies *in vivo*

(A) 5×10^6 parental and cetuximab-resistant OXCO-2 cells were injected subcutaneously into female nude mice. Following tumor growth for one week, treatment was initiated with ZM-447439 (ZM; 40 mg/kg) alone, cetuximab (Cmab; 0.8 mg) alone, or their combination by intraperitoneal (i.p.) injection at the times indicated by the arrows. Tumor volumes were calculated every other day (n=6 in each group). **(B)** Representative pictures of tumors at the end of the experiment in (A). **(C)** Representative cetuximab-resistant OXCO-2 tumors in the initial 5 days of treatment as in (A) were harvested, lysed, and analyzed for PUMA expression by western blotting. **(D)** TUNEL staining of the parental and cetuximab-resistant OXCO-2 tumors treated as in (C). *Left*, representative TUNEL staining pictures with arrows indicating example positive cells. Scale bars, 25 μm. *Right*, quantification of TUNEL signals. ***, $P<0.001$. **(E)** Active caspase-3 staining of the parental and cetuximab-resistant OXCO-2 tumors treated as in (C). *Left*, representative staining pictures with arrows indicating example positive cells. Scale bars, 25 μm. *Right*, quantification of active caspase-3 signals. ***, $P<0.001$.